Fabrication of core–shell hybrid nanoparticles by mineralization on poly(ε-caprolactone)-*b*-poly(methacrylic acid) copolymer micelles

Hong Jae Lee · Sang Cheon Lee

Abstract Polymer micelles containing calcium phosphate (CaP) minerals on the shell domain were developed by nanotemplate-driven mineralization. The polymer micelle nanotemplate was prepared by self-assembly of a poly(ε-caprolactone)-*b*-poly(methacrylic acid) (PCL-*b*-PMAA) copolymer. PMAA formed the anionic outer shell, and PCL constructed the hydrophobic inner core. Subsequent addition of calcium and phosphate ions to micellar solutions induced CaP mineral deposition within the PMAA shell domain. Transmission electron microscopy (TEM) showed the well-defined nanostructure consisting of the CaP nanoshell and the PCL inner core. Energy-dispersive X-ray spectroscopy (EDS) confirmed CaP deposition on polymer micelles. Dynamic light scattering (DLS) study showed CaP mineralization greatly enhanced the micellar stability.

Keywords Calcium phosphate · Mineralization · Nanoparticles · Polymer micelle

Introduction

Rational combination of inorganic species and organic nanostructured materials has provided an important guidance for the design of multifunctional hybrid nanomaterials [1, 2]. Recently, the deposition of inorganic components on self-assembled organic templates has broadened the choice of new functional nanoparticles [3, 4]. For example, the deposition of silica on core–shell polymer micelle templates was demonstrated by an inorganic sol–gel reaction on the micellar shells [5, 6]. This inorganic silicification could contribute to the

H. J. Lee · S. C. Lee (✉)
Department of Maxillofacial Biomedical Engineering and Institute of Oral Biology, School of Dentistry, Kyung Hee University, 1 Hoegi-dong, Dongdaemun-gu, Seoul 130-701, Korea
e-mail: schlee@khu.ac.kr

enhancement of micellar stability against dilution and micelle-disrupting chemicals. So far, polymer micelles have shown great potentials as intravenous targeted drug delivery systems [7–9]. However, they suffer from low structural stability and tend to disassemble upon injection into blood stream [10, 11]. For this reason, they can neither hold loaded drugs in the blood nor can preferentially release drugs within target cells. Therefore, the use of inorganic silica deposition is recognized as an intelligent approach to improve the stability of existing polymer micelles.

Another interesting class of hybrid nanoparticles is based on the mineralization of inorganic calcium phosphate (CaP) on self-assembled nanotemplates [2, 12]. In a previous report, the liposome-templated formation of CaP nanoshells was suggested as a useful approach to enhance the liposome stability by acting as a reinforcing coating [12]. CaP minerals have superiority to silica in terms of biocompatibility, because CaP is the main mineral components of natural bones [13]. Another feature that makes CaP more interesting is that it is absorbable at specific cellular environments (endosome/lysosome) as non-toxic ionic species [14]. Therefore, the combination of CaP mineralization with the rationally designed self-assembled nanotemplates would lead to the successful developments of robust, biocompatible nanoparticles, which can serve as a potential nanocarrier of drugs.

In this study, we describe CaP mineralization on self-assembled polymer micelles to produce highly robust hybrid nanoparticles. To prepare polymer micelle nanotemplates for mineralization, a self-assembling AB diblock copolymer of poly(ε-caprolactone)-*b*-poly(methacrylic acid) (PCL-*b*-PMAA) was synthesized. A detailed mineralization process in aqueous phase was described. TEM, DLS, and EDS analyses were carried out to characterize the mineralized nanoparticles. In addition, the effect of CaP mineralization on micellar stability against the severe micelle-disrupting condition was examined.

Experimental

Materials

tert-Butyl methacrylate (tBMA), trifluoroacetic acid (TFA), 1-pyrenebutyric acid, 1,3-dicyclohexylcarbodiimide (DCC), 4-dimethylaminopyridine, copper(I) bromide (Cu(I)Br, 99.999%), *N,N,N′,N′,N″*-pentamethyldiethylenetriamine (PMDETA), stannous octoate (Sn(Oct)$_2$), sodium dodecyl sulfate (SDS), and anhydrous magnesium sulfate were purchased from Aldrich Co. (Milwaukee, WI) and used without further purification. 2-Bromopropionyl bromide was purchased from Aldrich Co. (Milwaukee, WI) and freshly distilled under vacuum. ε-Caprolactone (CL) was purchased from Aldrich Co. (Milwaukee, WI), dried over calcium hydride, and vacuum distilled. Tetrahydrofuran (THF) and toluene were distilled from Na/benzophenone under N$_2$, prior to use. Calcium chloride (CaCl$_2$), disodium hydrogen phosphate (Na$_2$HPO$_4$), 35% hydrogen chloride (HCl), and sodium hydroxide (NaOH) were of the reagent grade.

Synthesis of pyrene-labeled poly(ε-caprolactone)-b-poly(methacrylic acid)
(Py-PCL-b-PMAA)

A fluorescent block copolymer was synthesized based on ring opening
polymerization and subsequent atomic transfer radical polymerization [15, 16].
In brief (i) synthesis of α-bromopropionyl-ω-hydroxy PCL (HO-PCL-Br), (ii)
pyrene-labeled PCL-b-poly-(tert-butyl methacrylate) (Py-PCL-b-PtBMA), and
(iii) hydrolysis of Py-PCL-b-PtBMA. For HO-PCL-Br, 2-hydroxyethyl
2′-bromopropionate (HEBP, 1.7 g, 0.009 mol) in dry toluene (40 mL) was dried
azeotropically, and CL (15 g, 0.13 mol) was added. After adding $Sn(Oct)_2$
(0.07 g, 0.17 mmol) at 120 °C, the polymerization was maintained under
nitrogen for 24 h. The HO-PCL-Br was isolated by precipitation in n-hexane
with a yield of 90%. To prepare Py-PCL-b-PtBMA, the HO-PCL-Br macroini-
tiator (1.5 g, 0.9 mmol) and Cu(I)Br (0.25 g, 3.5 mmol) were added to a flame-
dried round-bottomed flask. Toluene (5 mL) and tBMA were degassed by N_2 and
added to the flask, and then PMDETA (0.75 g, 3.5 mmol) was introduced. The
reaction temperature was maintained at 85 °C for 15 h. The block copolymers
were purified by passing through the silica gel column and precipitation from
THF into cold n-hexane. Pyrene was labeled at the terminal of the PCL block by
DCC chemistry. The block copolymers were denoted as Py-PCL-b-PtMBA.
Finally, the deprotection of Py-PCL-b-PtBMA was performed by treating the
block copolymers with TFA in methylene chloride. The final block copolymers
were denoted as Py-PCL-b-PMAA. Block composition and number average
molecular weight were calculated by ^{1}H NMR spectroscopy recorded at
400 MHz on a Varian INOVA400 NMR spectrometer.

Mineralization of core–shell–corona polymer micelles

For calcium phosphate mineralization on Py-PCL-b-PMAA polymer micelles, an
aqueous $CaCl_2$ solution (0.1 mL, 2.9 mM) was added to aqueous polymer micelles
(0.9 mL, 1 g/L) at pH 7.0 and equilibrated for 5 h under stirring at 400 rpm. The
molar concentration ratios of [MAA] to [calcium ion] were 1:0.5. An aqueous
solution of Na_2HPO_4 (0.2 mL, 2.9 mM) was slowly added to the reaction mixture,
and the solution was stirred at 400 rpm at room temperature for 10 h. The solution
was dialyzed to remove unreacted ionic species, and the dialyzate was lyophilized to
obtain the mineralized hybrid nanoparticles.

Stability of mineralized micelles

Kinetic stability of non-mineralized and mineralized micelles was investigated by
adding SDS. The effect of SDS on mineralized micelles was estimated by dynamic
light scattering analysis. A SDS solution (1 mL, 7.5 g/L) was added to the
mineralized micelle solution (2 mL, 0.75 g/L), and the solution was stirred at
400 rpm. Time-dependent scattered light intensity was monitored by dynamic light
scattering.

Fluorescence measurements

Pyrene excitation spectra were recorded on a JASCO FP-6500 spectrofluorometer. For the measurement of excitation spectra, emission and excitation band widths were set at 5 and 1 nm, respectively. The emission wavelength was 390 nm, and the excitation spectra were recorded in the wavelength range of 300–380 nm. The spectra were accumulated with an integration of 3 s/nm.

Light scattering measurements

Dynamic light scattering measurements were performed using a 90 Plus particle size analyzer (Brookhaven Instruments Corporation). The sample solutions were purified by passing through a Millipore 0.45 μm filter. The scattered light of a vertically polarized He–Ne laser (632.8 nm) was measured at an angle of 90° and was collected on an autocorrelator. The mean diameters (d) of mineralized and non-mineralized micelles were calculated by using the Stokes–Einstein equation $d = k_{B}T/3\pi\eta D$, where k_{B} is the Boltzmann constant, T is the absolute temperature, η is the solvent viscosity, and D is the diffusion coefficient.

Zeta potential

Zeta potentials were measured using a BrookHAVEN Instruments Cooperation 90 PLUS (New York, USA) particle size analyzer. Aqueous solutions (1 mg/mL) of non-mineralized and mineralized micelles were prepared and measured separately at pH 7.4.

Transmission electron microscopy (TEM)

TEM was performed on a JEM-2000EX (JEOL Tokyo, Japan), operating at an acceleration voltage of 200 kV. For sample preparation, a drop of sample solution (concentration = 1 g/L) was placed onto a 200-mesh copper grid coated with carbon. About 3 min after deposition, the grid was tapped with a filter paper to remove surface water, followed by air-drying. Non-mineralized polymer micelles were stained with uranyl acetate (1 wt%). Mineralized polymer micelles were observed without a staining process.

TEM-associated energy-dispersive X-ray photoelectron spectroscopy (EDS)

EDS measurement was carried out using JEOL JEM-2100F equipped with an EDAX Genesis Series-TEM at 200 kV. The mineralized area on the micelles was analyzed by EDS.

Results and discussion

A self-assembling diblock copolymer (Py-PCL-*b*-PMAA) was used as a nanotemplate for calcium phosphate mineralization (Fig. 1). For calculation of molar composition ratio in the block copolymer, the number average molecular weight (M_n) of HO-PCL-Br could first be calculated. Using peak integration ratio of C*H* in the 2-bromopropionate initiator end group at 4.63 ppm to C*H*$_2$ protons in the PCL repeating unit at 3.97 ppm, we could calculate accurately the repeating units of PCL. Finally, the number average molecular weight of each block in Py-PCL-*b*-PMAA was calculated by the peak integration ratio of (C*H*$_3$)$_3$ protons in –CH$_2$(CH$_3$)CHCOOC–(CH$_3$)$_3$– of PtBMA at 1.44 ppm and C*H*$_2$ protons in –CO(CH$_2$)$_4$CH$_2$O– of the PCL repeating unit at 3.97 ppm. The molar composition ratio of repeating units in PCL and PMAA was 29:30. Pyrene was labeled to monitor the assembly behavior in an aqueous phase.

The amphiphilic Py-PCL-*b*-PMAA self-assembled to form the polymer micelle with two well-defined, distinct domains: the hydrophobic PCL inner core and the anionic PMAA outer shell. The polymer micelle has a mean diameter of 65.5 nm with a narrow size distribution (polydispersity factor = 0.06) in the phosphate buffered saline (PBS) solution. The critical micelle concentration (cmc) of the block copolymer in PBS (pH 7.4), estimated by pyrene excitation spectra, was 18 mg/L. The zeta potential (ζ) of Py-PCL-*b*-PMAA micelles was reasonably negative ($\zeta = -29.25$ mV).

The PMAA middle shell can serve as a spatial domain for mineralization of inorganic CaP nanoshells. CaP deposition on polymer micelle assemblies was initiated by electrostatic localization of calcium ions at anionic MAA moieties. Subsequent addition of the phosphate anion source induced the formation of double ionic layers within the PMAA middle shells, thereby increasing the ionic concentration above the critical saturation point to trigger the nucleation and growth of nanophase CaP. The molar ratio of [MAA]/[calcium ion] was fixed at 1:0.5 to prevent CaP nucleation in an aqueous phase and selectively induce mineral deposition on the acidic PMAA shells. The non-mineralized polymer micelle and the mineralized polymer micelle are denoted as NPM and CaP-PM, respectively. Figure 2a and b shows the TEM images of NPM and CaP-PM. It is interesting to note that CaP-PM ((b)) can be visualized as a dark nano-circle of uniform diameter even without staining, whereas NPM (a) can be observed only with negative staining. This reflects the formation of inorganic nanoshells on the polymer micelle
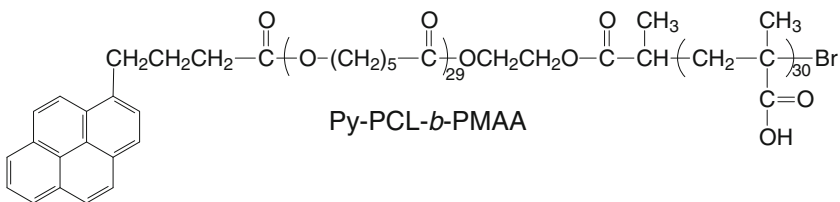

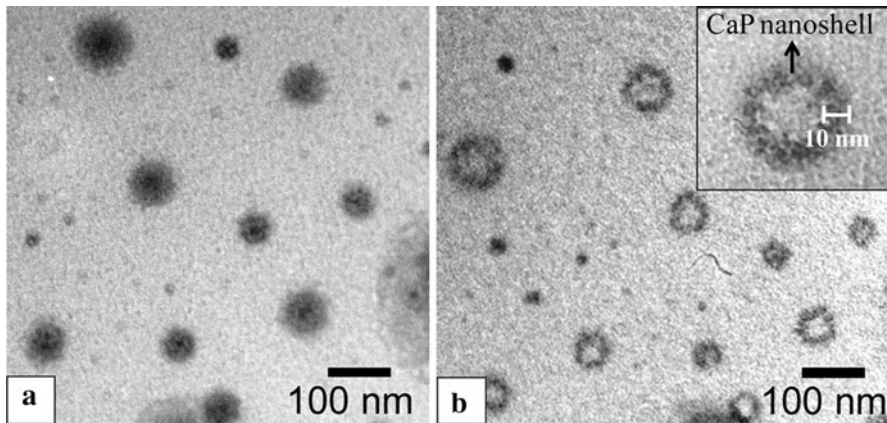**Fig. 1** Chemical structure of Py-PCL-*b*-PMAA copolymer

Fig. 2 TEM images of NPM (negatively stained) (**a**) and CaP-PM (unstained) (**b**)

nanotemplate. The shell thickness was estimated to be 10 nm. The mean diameter of CaP-PM in PBS (pH 7.4) solution was 60.0 nm, and the mineralized polymer micelles maintain the size of template micelles (Fig. 3a, b; Table 1). It is noteworthy that the zeta potentials of the polymer micelles ($\zeta = -29.25$) increased up to around -3.0 after mineralization. This indicates that the mineral deposition on PMAA shells shielded anionic carboxylate charges. Energy-dispersive X-ray spectroscopy (EDS) confirmed that CaP-PM exhibited Ca and P atomic elements, which belonged to CaP minerals (Fig. 4).

Mineralized CaP nanoshells may affect the polarity of inner core, since it can protect the diffusion of water toward PCL core regions. Pyrene labeled at the terminus of PCL is embedded within the PCL micellar core, and its fluorescence may monitor the change of environmental polarity of core regions [17]. Figure 5 shows the pyrene excitation spectra before or after mineralization. It is noteworthy that λ_{max} of pyrene bands shifts from 334 to 347 nm, reflecting that CaP deposition greatly decreases the inner core polarity, probably by protecting the access of water molecules. Besides, the CaP nanoshell may hold the self-assembled structures and hinder rotational freedom of polymer chains. This suggests that the controlled
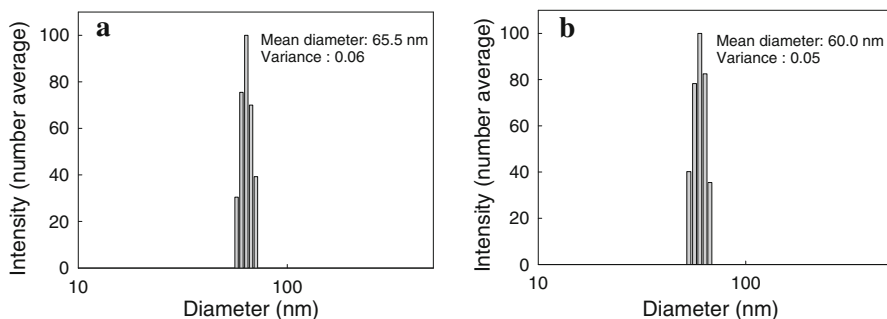

Fig. 3 Size distributions of NPM (**a**) and CaP-PM (**b**) in PBS (pH 7.4) by dynamic light scattering

Table 1 Zeta potentials, mean hydrodynamic diameters, and polydispersity factors of various micelles

Nanoparticles	d^a (nm)	Zeta potential^b (mV)	μ_2/Γ^{2c}
NPM	65.5	−29.25	0.06
CaP-PM	60.0	−3.0	0.05

[a] Mean hydrodynamic diameter in PBS pH 7.4

[b] Estimated at pH 7.4 at 25 °C

[c] Polydispersity factor determined by dynamic light scattering

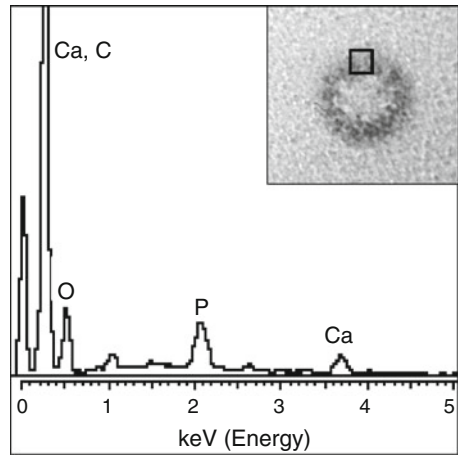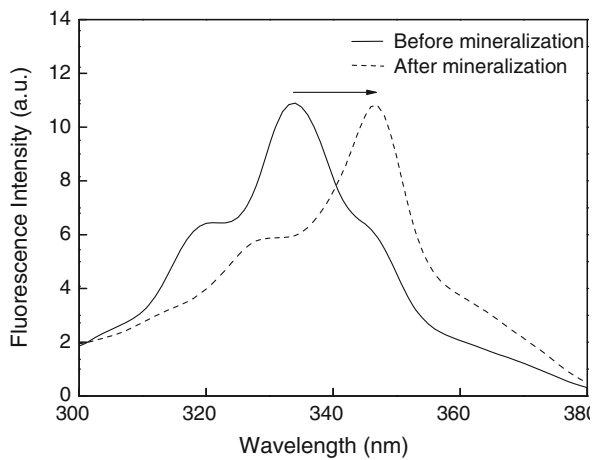**Fig. 4** EDS analysis data of mineralized CaP nanoshells

**Fig. 5** Pyrene excitation spectra of aqueous NPM (before mineralization) and CaP-PM (after mineralization)

deposition of CaP on the micellar shells can modulate the diffusion of low molecular weight compounds.

In the field of drug delivery, the robustness of micelles is an issue of great importance since it can determine the delivery efficiency of nanocarriers. When they are subjected to the severe condition of dilution in blood or interaction with biological lipids, they tend to lose structural integrity and finally dissociate [10, 11]. Thus, we investigated whether the CaP nanoshells can act as a micellar shell cross-linker, thereby enhancing the stability of polymer micelles. The kinetic stability of NPM and CaP-PM was examined in the presence of SDS, a strong micellar destabilizing agent [7, 18]. After adding aqueous SDS to the solutions of each micelle system, the relative intensity of scattering light (SLI/SLI_0) was monitored (Fig. 6). For NPM, a drastic decrease in scattered light intensity was observed within 30 min, and SLI/SLI_0 reached approximately 65% after 3 h. A dynamic autocorrelation fitting for reliable measurements of micelle sizes could not be obtained, and particle sizes and polydispersity could not be obtained. This reflects the SDS-induced permanent dissociation of the majority of polymer micelles. [18]. In contrast, CaP-PM exhibited enhanced stability displaying minimal decreases in scattering intensities by maintaining the initial value over 90% for up to 3 h. In addition, the nanoparticle size remained unchanged. After 3 h, the micelle size was 60.5 nm with narrow size distribution. This result indicates that the mineralized CaP nanoshells effectively hold micellar assemblies to enhance structural stability.

Currently, shell cross-linking approaches for enhancing micellar stability are mostly based on organic cross-linkers, of which body toxicity has not been well defined [19]. CaP minerals on polymer micelles are superior to current organic cross-linkers in that CaP is naturally formed and can be absorbable in body as non-toxic ions such as calcium and phosphate ions.

Fig. 6 Kinetic changes in relative scattered light intensity (SLI/SLI_0) for aqueous NPM and CaP-PM
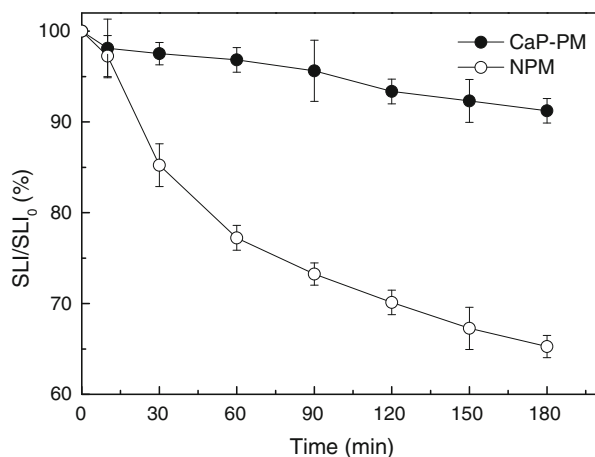
Conclusions

A novel organic–inorganic hybrid nanoparcticle was prepared based on nanotempate-driven domain-specific CaP deposition. The CaP nanoshell with a uniform thickness was successfully assembled on the anionic outer domain of PCL-*b*-PMAA polymer micelles. CaP minerals could strongly hold the self-assembled micellar structure, thereby enhancing the robustness of polymer micelles. Since CaP is known to be absorbable in intracellular environments, mineralized polymer micelles may express the features of ideal targeted nanocarriers by showing enhanced carrier stability as well as selective drug release within cells. Besides, CaP nanocapsules can be fabricated simply by eliminating PCL inner cores using a base treatment. The mineralization technology described in this study may provide a platform technology for the generation of many useful functional nanoparticles.

References

1. Pouget E, Dujardin E, Cavalier A, Moreac A, Valéry C, Marchi-Artzner V, Weiss T, Renault A, Paternostre M, Artzner F (2007) Hierarchical architectures by synergy between dynamical template self-assembly and biomineralization. Nat Mater 6:434–439
2. Schmidt HT, Ostafin AE (2002) Liposome directed growth of calcium phosphate nanoshells. Adv Mater 14:532–535
3. Hartgerink JD, Beniash E, Stupp SI (2001) Self-assembly and mineralization of peptide-amphiphile nanofibers. Science 294:1684–1688
4. Huo Q, Liu J, Wang LQ, Jiang Y, Lambert TN, Fang E (2006) A new class of silica cross-linked micellar core-shell nanoparticles. J Am Chem Soc 128:6447–6453
5. Khanal A, Inoue Y, Yada M, Nakashima K (2007) Synthesis of silica hollow nanoparticles templated by polymeric micelle with core-shell-corona structure. J Am Chem Soc 129:1534–1535
6. Yuan JJ, Mykhaylyk OO, Ryan AJ, Armes SP (2007) Cross-linking of cationic block copolymer micelles by silica deposition. J Am Chem Soc 129:1717–1723
7. Koo AN, Lee HJ, Kim SE, Chang JH, Park C, Kim C, Park JH, Lee SC (2008) Disulfide-cross-linked PEG-poly(amino acid)s copolymer micelles for glutathione-mediated intracellular drug delivery. Chem Commun 48:6570–6572
8. Lee SC, Huh KM, Lee J, Cho YW, Galinsky RE, Park K (2007) Hydrotropic polymeric micelles for enhanced paclitaxel solubility: in vitro and in vivo characterization. Biomacromolecules 8:202–208
9. Lee Y, Park SY, Mok H, Park TG (2008) Synthesis, characterization, antitumor activity of pluronic mimicking copolymer micelles conjugated with doxorubicin via acid-cleavable linkage. Bioconjugate Chem 19:525–531
10. Lee SW, Chang DH, Shim MS, Kim BO, Kim SO, Seo MH (2007) Ionically fixed polymeric nanoparticles as a novel drug carrier. Pharm Res 24:1508–1516
11. Ko J, Park K, Kim YS, Kim MS, Han JK, Kim K, Park RW, Kim IS, Song HK, Lee DS, Kwon IC (2007) Tumoral acidic extracellular pH targeting of pH-responsive MPEG-poly(β-amino ester) block copolymer micelles for cancer therapy. J Control Rel 123:109–115
12. Schmidt HT, Gray BL, Wingert PA, Ostafin AE (2004) Assembly of aqueous-cored calcium phosphate nanoparticles for drug delivery. Chem Mater 16:4942–4947
13. Kim SE, Choi HW, Lee HJ, Chang JH, Choi J, Kim KJ, Lim HJ, Jun YJ, Lee SC (2008) Designing a highly bioactive 3D bone-regenerative scaffold by surface immobilization of nano-hydroxyapatite. J Mater Chem 18:4994–5001

14. Kakizawa Y, Furukawa S, Kataoka K (2004) Block copolymer-coated calcium phosphate nanoparticles sensing intracellular environment for oligodeoxynucleotide and siRNA delivery. J Control Rel 97:345–356

15. Lee SC, Kim KJ, Jeong YK, Chang JH, Choi J (2005) pH-Induced reversible complexation of poly(ethylene glycol) and poly(ε-caprolactone)-b-poly(methacrylic acid) copolymer micelles. Macromolecules 8:9291–9297

16. Lee SC, Lee HJ (2007) pH-Controlled, polymer-mediated assembly of polymer micelle nanoparticles. Langmuir 23:488–495

17. Wilhelm M, Zhao CL, Wang Y, Xu R, Winnik MA, Mura JL, Riess G, Croucher MD (1991) poly(Styrene-ethylene oxide) block copolymer micelle formation in water: a fluorescence probe study. Macromolecules 24:1033–1040

18. Kang N, Perron MÈ, Prud'homme RE, Zhang Y, Gaucher G, Leroux JC (2005) Stereocomplex block copolymer micelles: core-shell nanostructures with enhanced stability. Nano Lett 5:315–319

19. Read ES, Armes SP (2007) Recent advances in shell cross-linked micelles. Chem Commun 3021–3035